# Gain and Distortion Optimization for Fast-Startup AC-Coupled Baseband Amplifiers in Motion-Sensing Radar

Aaron B. Carman, Christopher Williams, and Changzhi Li

Department of Electrical and Computer Engineering, Texas Tech University, Lubbock, TX, USA aaron.b.carman@ttu.edu

Abstract—Microwave radar has been widely adopted as a wireless sensor to accurately detect µm-scale motions. Lowcost sensors often use ac-coupled baseband amplifiers to increase the signal level for digitization, but these can increase startup times for low-frequency sensing. Recent architectures have shown that startup times can be improved using commercial diodes but have not been tested in a wide range of use cases to evaluate potential limitations. This work presents an in-depth analysis of diode-based ac-coupled fast-startup amplifiers to quantify the impacts of 2<sup>nd</sup> order effects on amplifier performance. The closed-form solutions are verified using SPICE software, with experimental results confirming the effects of nonidealities in realistic radar applications.

### Keywords—baseband amplifiers, distortion, fast-startup

# I. INTRODUCTION

As wireless sensor technology continues to advance, microwave radar sensors have seen considerable use as a method of detecting miniscule motions [1]. Especially in human-aware sensing, radars are used in cases such as Fig. 1 where a microwave sensor could monitor vital signs [2, 3] or in other applications such as wireless structural health monitoring [4, 5]. The radar sensor's output signals consist of dc information produced by clutter and electronic biasing and ac information produced by motion [6]. Oftentimes this ac information is orders of magnitude smaller than the dc level, requiring ac-coupled amplifiers or dc-coupled systems to prevent saturation at the amplifier output. DC-coupled systems have low distortion compared to ac-coupled systems due to the lack of high-pass capacitors, but are typically more complex and costly [7–9]. AC-coupled systems, on the other hand, typically require large values of resistors and capacitors to avoid distortion which increases the startup times considerably, shown in Fig. 1(a) [10]. Recently, new low-cost ac-coupled baseband amplifier architectures for low-frequency measurements have exhibited a faster startup time leveraging commercial diodes [10-12]. Ideally, these architectures present no distortion, and result in a startup improvement illustrated by Fig. 1(b). At extremely low frequencies, however, parasitic effects can introduce distortion such as that in Fig. 1(c). These architectures have so far not been rigorously modeled mathematically, nor have the impacts of amplifier parameters such as gain or offset voltage been considered. As a result, the utility and limitations of the fast-start amplifier are currently unknown.

The authors wish to acknowledge the National Science Foundation (NSF) for funding support under Grant ECCS-2030094 and CIS-2112003.

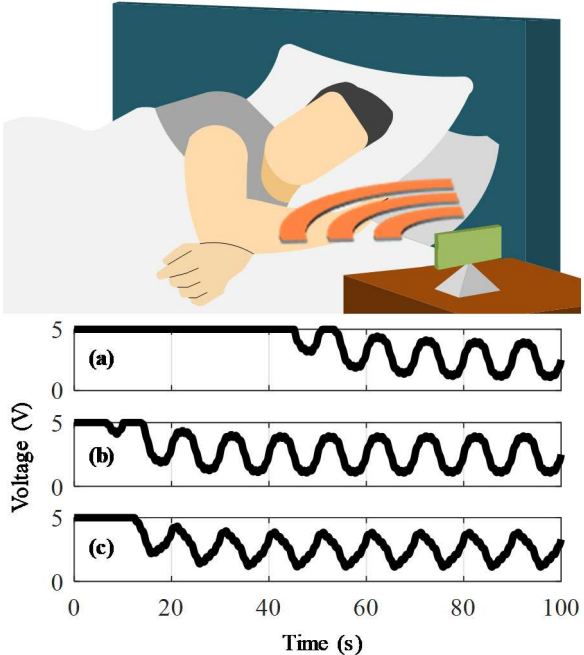


Fig. 1. Example radar application and effects of fast-startup amplifiers. Compared to the traditional case (a), an ideal fast-startup improves start time (b), but can unintentionally distort the resulting signal in a real case (c).

This paper presents an improved model for the diodebased ac-coupled baseband amplifier to determine the impacts of gain, offset voltage, and diode characteristics on transient and frequency-domain performance of the resulting amplifier. Section II describes the models used to characterize these effects in both the time- and frequencydomains. Section III then evaluates these effects experimentally using a bench-level test and a realistic application with a 120-GHz radar sensor. Conclusions are drawn in Section IV along with a discussion on future works.

# II. AMPLIFIER MODELING

Two models are developed to model the transient and frequency-domain responses of the amplifier first presented in [11]. For the following analyses, it is assumed that no signal is present for transient analysis, while for frequency-domain analysis it is assumed that the amplifier has reached a steady-state equilibrium. The amplifier response can then be considered as a superposition of the two models.

# A. Startup Model

The diode-based fast-start amplifier architecture functions by providing a low-resistance path to charge the

input capacitors present in low-frequency baseband amplifiers, greatly accelerating the startup time [10]. The diodes cannot fully charge the capacitor immediately, however. Once the capacitor voltage is within the diodes' forward voltage  $V_F$ , charging is accomplished primarily through the RC circuit consisting of the combination of amplifier input impedance  $R_{\rm in}$  and diode parasitic resistance  $R_D$ , and the input capacitor  $C_{\rm in}$ . If it is assumed that the diode very rapidly charges  $C_{\rm in}$  within its forward voltage, the capacitor transient voltage can be approximated as

$$v_c(t) = V_b - V_F e^{-\frac{t}{\eta R_{\text{eff}} C_{\text{in}}}} - V_{OS} \tag{1}$$

where  $V_b$  is the bias voltage that sets the dc level of the output,  $V_{OS}$  is the amplifier input offset voltage,  $R_{eff}$  =  $R_{\rm in}||R_D$  is the effective input resistance, and  $\eta$  is a corrective factor to account for the nonzero diode current draw while charging [13]. A simple one-stage amplifier model is shown in Fig. 2 that illustrates the impact of the various parameters. It is worth noting that the parameter  $V_F$ is not a fixed value as there is no ideal "cutoff" voltage. As a result, the quiescent current should be considered during the design process to determine an appropriate value of  $V_E$ . In this case, a value of 100 mV is used as this ensures that the current through the RB520CM-60 diode is negligible compared to the RC currents. Typically,  $V_b$  is set to half of  $V_{DD}$  to provide maximum dynamic range at the amplifier output. The baseband amplifier is then modeled as a differential amplifier that amplifies the difference between (1) and  $V_b$  with a gain of  $A_V$ . This difference and resulting output voltage can be written using (2) and (3), respectively.

$$v_{\rm err}(t) = v_{C}(t) - V_{b} = -V_{F}e^{-\frac{t}{\eta R_{\rm eff}C_{\rm in}}} - V_{OS}$$
 (2)

$$v_O(t) = -A_V V_F e^{-\frac{t}{\eta R_{\text{eff}} C_{\text{in}}}} - A_V V_{OS} + V_b$$
 (3)

Since (3) is limited by the supply voltage of the amplifier, limiting values of  $v_{\rm err}$  can be found by restricting  $v_{\it o}$  between these limits. If  $v_{\rm err}$  exceeds these bounds, the amplifier output is saturated and will not output useful data. After algebraic manipulation, a closed-form approximation for start-time can be found in (4) if  $V_{\it b} = V_{\it DD}/2$ .

$$t_S = -\eta R_{\rm eff} C_{\rm in} \ln \left( \frac{V_b + A_V V_{OS}}{A_V V_F} \right) \tag{4}$$

In addition to determining the start time, it is also critical that the final value of the amplifier output approaches a value within the voltage range of the system. Otherwise, the amplifier will be saturated and will never provide accurate outputs. From (3),  $V_{OS}$  is found to produce a steady-state error in the amplifier output which must be considered. If it is assumed that  $V_b = V_{DD}/2$ , the maximum value of gain

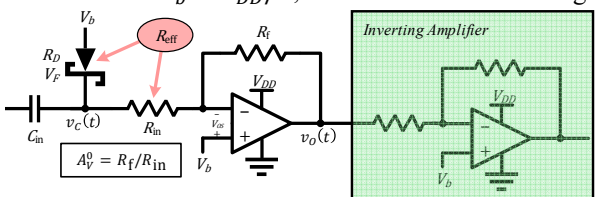


Fig. 2. Amplifier model. The diode parameters, offset voltage, and amplifier gain impact start time, while the parasitic diode resistance can increase the lower cutoff frequency and introduce distortion.

can be found which will allow the output to settle to a point that does not saturate the amplifier in (5).

$$|A_{V_{\text{max}}}| = \frac{V_b}{V_{OS}} \tag{5}$$

From (4) and (5), the effects of gain can be determined. Intuitively, as  $A_V$  increases, the maximum allowable value of  $v_{\rm err}$  decreases which therefore increases the start-time. To determine the accuracy of (4) and (5), a SPICE simulation is used to evaluate the realistic start-time which is then compared to the approximation from (4). In addition, the analysis is restricted to gain values where the amplifier can start to determine the accuracy of (5). The results of this are shown in Fig. 3(a), where the startup time in three cases shows good agreement with the closed-form solution. It is worth noting that each case settles to a different final dc value because of the input offset voltage introducing dc error that is amplified by the following stages. (4) is then evaluated for a range of gain values, where an increase in baseband gain is seen to heavily impact the startup time or prevent the amplifier from starting as shown in Fig. 3(b).

### B. Amplifier AC Model

To study distortion effects, an ac model is developed to predict the amplifier output based on input port characteristics. The proposed model assumes that the accoupling is a result of a single capacitor at the input of the amplifier and that the amplifier provides a gain of  $A_V^0$ . Using the model in Fig. 2, the combination of  $Z_C = -j/\omega C_{\rm in}$  and  $R_{\rm eff}$  are seen to create the high-pass behavior present in accoupled amplifiers while the inverting amplifier provides gain. The overall transfer function as a function of frequency can be written as (6).

$$A_V(f) = \frac{A_V^0 R_{\text{eff}}}{Z_C + R_{\text{eff}}} \tag{6}$$

In addition to providing a faster start time, the inclusion of fast-start diodes changes the frequency-domain characteristics of the amplifier by changing  $R_{\rm eff}$ . This is a result of the nonzero resistance of the diodes, which can load the input and increase the cutoff frequency of the amplifier.

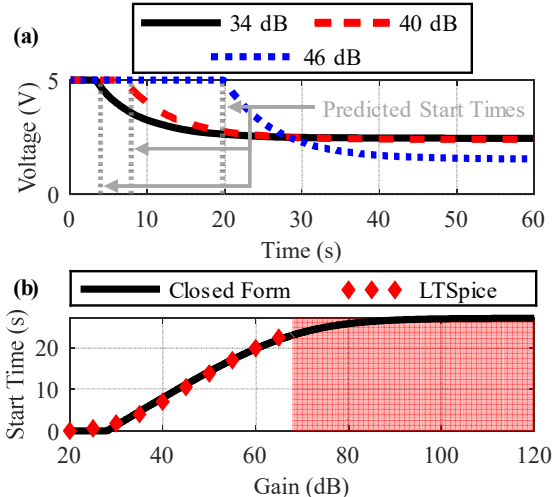


Fig. 3. Comparison of closed-form and SPICE solutions. The time-domain results (a) show good agreement, while the results versus gain (b) highlight the model's accuracy across multiple values of gain.

This is evaluated first using the closed-form equation in (6) and with SPICE software across a range of frequencies. The diodes considered are the RB520CM-60 Schottky diodes from ROHM, which have been previously shown in [10] to offer a good tradeoff between ac-performance and startup time. The input capacitance is set as  $10~\mu\text{F}$  while the input resistance of the amplifier  $R_{\text{in}}$  is set to  $10~\text{M}\Omega$ . In addition, the diode small-signal resistance  $R_D$  is measured using SPICE software and is found to be approximately 699 k $\Omega$ . The ideal gain  $A_V^0$  is set to 100~V/V (40 dB) by tuning the inverting amplifier stages following the fast-startup circuit.

The results from the ac analysis before and after adding diodes are shown in Fig. 4. Without including fast-start diodes, R<sub>eff</sub> consists only of the input resistance of the amplifier. As a result, a very low cutoff frequency can be obtained at the cost of a long startup time. This low cutoff frequency of 0.0016 Hz can be seen in Fig. 4, where the closed-form (solid curve) and SPICE solutions (diamonds) show good agreement. If diodes are included to help reduce the start time, their impact on the amplifier's ac response must also be considered. After including the diodes,  $R_{\rm eff}$ now consists of both  $R_{\rm in}$  and  $R_{\rm D}$  in parallel, reducing the value of  $R_{\rm eff}$  compared to the case with no diodes. The values of  $A_V$  over the same frequency range are shown in Fig. 4, where the closed-form (dashed curve) and SPICE solutions (crosses) show that the cutoff frequency has been considerably reduced to 0.024 Hz. As a result, the effect of fast-start diodes must be carefully considered when developing low-frequency amplifiers.

## III. EXPERIMENTAL RESULTS

To evaluate the gain-dependence and distortion introduced by fast-start diodes, two experiments are developed. The first leverages a bench-level setup to evaluate the impacts of gain on start times under the same conditions. The second experiment implements the fast-start amplifier in a 120-GHz interferometric radar system to precisely measure motion, where the impacts of distortion introduced by fast-start diodes can be evaluated in a realistic sensing setup.

# A. Gain-Dependence Experiment

To experimentally determine the impacts of gain on start time, fast-start amplifiers based on the RB520CM-60 Schottky diodes are used with varying values of gain. After a power-on event, the output voltage of each amplifier is recorded to determine the start time. In this experiment, the gain is controlled solely by changing the gain of the inverting amplifier stages following the fast-startup circuits to not have an unintended impact on startup by modifying  $R_{\rm eff}$ . The input in all cases is connected to a 10 mV<sub>P-P</sub> 0.1 Hz sine wave

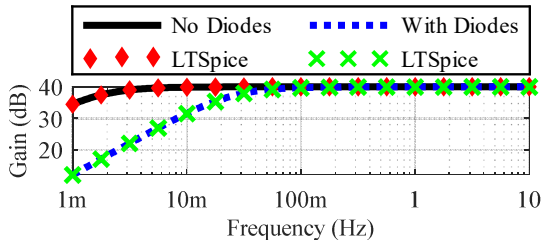


Fig. 4. Comparison of frequency-domain results. Across the range of interest, the closed-form solutions (solid and dashed curves) show good agreement with SPICE simulations (diamond and cross markers).

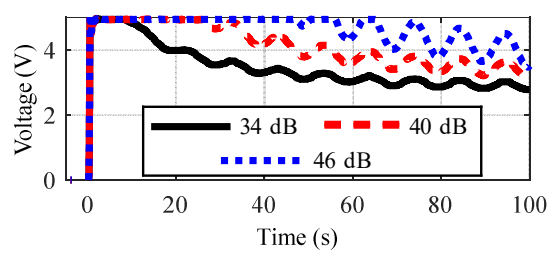


Fig. 5. Startup times with varying gain values. With higher gain values the associated startup time increases, requiring in-depth evaluation to determine the suitability of the architecture in low-frequency applications.

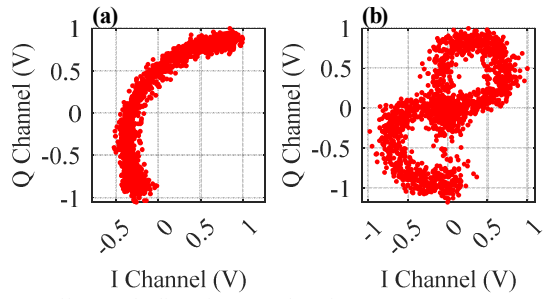


Fig. 6. Effects of distortion on low-frequency measurement. The constellation plot shows little distortion without diodes (a) and much greater distortion with diodes (b) as a result of the lower effective resistance.

created by a function generator. The results of this study are shown in Fig. 5. From the results, it is seen that higher gain values naturally accompany a longer startup time. As a result, the proposed fast-start circuit should be evaluated in each specific application to determine if the startup time is sufficient when using realistic values of gain.

# B. Radar-Based Distortion Experiment

To evaluate the impacts of distortion, a traditional and a fast-startup amplifier is implemented along with two commercial 120-GHz radar modules [14]. This allows for evaluation of the distortion effects under similar conditions. The radars are placed 1.5 m away from a corner reflector moving with 0.5 Hz motion frequency and 0.5 mm peak-to-peak amplitude. The results of this experiment are shown in Fig. 6. Without diodes, the startup time is increased but the resulting motion exhibits very little distortion, as is shown in Fig. 6(a) where the output occupies an arc on the unit circle. After adding diodes, the increased cutoff frequency introduces distortion shown in Fig. 6(b) where the results appear in a bowtie pattern that is characteristic of decoupling distortion in motion sensing radars [15, 16].

# IV. CONCLUSION

This paper presented an analysis of gain and distortion effects introduced in fast-startup ac-coupled baseband amplifiers. Two models for amplifier startup time and frequency performance are derived and compared against commercial simulations where it is shown that start-time and frequency response can be accurately calculated. The models are then verified experimentally using a benchtop setup where it is seen that amplifier gain can impact startup times considerably. In addition, a radar-based experiment shows that distortion can impact low-frequency measurements. Future works should continue to develop the amplifier model to consider nonidealities such as input capacitance and work toward developing fast-startup amplifiers which do not introduce steady-state distortion.

### REFERENCES

- F. Fioranelli and J. Le Kernec, "Radar sensing for human healthcare: challenges and results," in 2021 IEEE Sensors, Oct. 2021, pp. 1–4.
- [2] A. Sinharay, R. Das, and S. Seth, "A Novel Microwave Measurement Technique for Non-Contact Vital Sign Monitoring," in 2018 IEEE SENSORS, Oct. 2018, pp. 1–4.
- [3] S. Izumi et al., "Non-contact Atrial Fibrillation Detection using a 24-GHz Microwave Doppler Radar," in 2022 IEEE Sensors, Oct. 2022, pp. 1–4.
- [4] D. V. Q. Rodrigues, D. Zuo, and C. Li, "Wind-Induced Displacement Analysis for a Traffic Light Structure Based on a Low-Cost Doppler Radar Array," *IEEE Trans. Instrum. Meas.*, vol. 70, pp. 1–9, 2021.
- [5] S. Guan, J. A. Rice, C. Li, and C. Gu, "Automated DC Offset Calibration Strategy for Structural Health Monitoring Based on Portable CW Radar Sensor," *IEEE Trans. Instrum. Meas.*, vol. 63, no. 12, pp. 3111–3118, Dec. 2014.
- [6] I.-S. Lee, J.-H. Park, and J.-R. Yang, "Detrending Technique for Denoising in CW Radar," *Sensors*, vol. 21, no. 19, p. 6376, Sep. 2021.
- [7] Z. Peng, A. Mishra, J. R. Davis, J. A. Bridge, and C. Li, "Long-time non-contact water level measurement with a 5.8-GHz DC-coupled interferometry radar," in 2018 IEEE International Instrumentation and Measurement Technology Conference (I2MTC), May 2018, pp. 1–5.
- [8] D. Tang, J. Wang, W. Hu, Z. Peng, Y.-C. Chiang, and C. Li, "A DC-Coupled High Dynamic Range Biomedical Radar Sensor With Fast-Settling Analog DC Offset Cancelation," *IEEE Trans. Instrum. Meas.*, vol. 68, no. 5, pp. 1441–1450, May 2019.

- [9] D. Tang, J. Wang, Z. Peng, Y.-C. Chiang, and C. Li, "A DC-coupled biomedical radar sensor with analog DC offset calibration circuit," in 2018 IEEE International Instrumentation and Measurement Technology Conference (I2MTC), May 2018, pp. 1–6.
- [10] A. B. Carman and C. Li, "Low-Cost Fast-Start Amplifier Architecture for AC-Coupled Measurement of Low-Frequency Signals," *IEEE Sens. Lett.*, vol. 8, no. 5, pp. 1–4, May 2024.
- [11] A. B. Carman and C. Li, "Passive Multistatic Wireless Sensing Based on Discrete LNA/Mixer Co-Optimization and Fast-Startup Baseband Amplifier," in 2023 IEEE Topical Conference on Wireless Sensors and Sensor Networks, Jan. 2023, pp. 43–45.
- [12] A. B. Carman and C. Li, "A Digital Beamforming Fast-Start Passive Radar for Indoor Motion Detection and Angle Estimation," *IEEE Trans. Microw. Theory Tech.*, pp. 1–12, 2024.
- [13] C. Alexander and M. Sadiku, Fundamentals of Electric Circuits, 6th ed. New York, NY: McGraw-Hill Education, 2017.
- [14] Indie Semiconductor, "TRA\_120\_002 Datasheet," Indie Semiconductor. Accessed: May 21, 2024. [Online]. Available: https://downloads.ffo.indiesemi.com/datasheets/Datasheet\_TRA\_12 0 002 V0.8.pdf
- [15] C. Gu, Z. Peng, and C. Li, "High-Precision Motion Detection Using Low-Complexity Doppler Radar With Digital Post-Distortion Technique," *IEEE Trans. Microw. Theory Tech.*, vol. 64, no. 3, pp. 961–971, Mar. 2016.
- [16] D. Rodriguez and C. Li, "Sensitivity and Distortion Analysis of a 125-GHz Interferometry Radar for Submicrometer Motion Sensing Applications," *IEEE Trans. Microw. Theory Tech.*, vol. 67, no. 12, pp. 5384–5395, Dec. 2019.